

# Electrovacuum Static Counter-Rotating Relativistic Dust Disks

Gonzalo García R.\* and Guillermo A. González†  
*Escuela de Física, Universidad Industrial de Santander*  
*A.A. 678, Bucaramanga, Colombia*

October 30, 2018

## Abstract

A detailed study of the Counter-Rotating Model (CRM) for generic electrostatic (magnetostatic) axially symmetric thin disks without radial pressure is presented. We find a general constraint over the counter-rotating tangential velocities needed to cast the surface energy-momentum tensor of the disk as the superposition of two counter-rotating charged dust fluids. We then show that this constraint is satisfied if we take the two counter-rotating streams as circulating along electrogeodesics with equal and opposite tangential velocities. We also find explicit expressions for the energy densities, electrostatic (magnetostatic) charge densities and velocities of the counter-rotating fluids. Three specific examples are considered where we obtain some CRM well behaved based in simple solutions to the Einstein-Maxwell equations. The considered solutions are Reissner-Nordström in the electrostatic case, its magnetostatic counterpart and two solutions obtained from Taub-NUT and Kerr solutions.

PACS numbers: 04.20.-q, 04.20.Jb, 04.40.-b

## 1 Introduction

Stationary or static axially symmetric exact solutions of Einstein equations describing relativistic thin disks are of great astrophysical importance since can be used as models of certain stars, galaxies, accretion disk and universes. Theses were first studied by Bonnor and Sackfield [1], obtaining pressureless static disks, and then by Morgan and

---

\*e-mail: gogarcia@uis.edu.co

†e-mail: guillego@uis.edu.co

Morgan, obtaining static disks with and without radial pressure [2, 3]. In connection with gravitational collapse, disks were first studied by Chamorro, Gregory and Stewart [4]. Disks with radial tension have been also recently studied [5]. Several classes of exact solutions of the Einstein field equations corresponding to static and stationary thin disks have been obtained by different authors [6 – 16], with or without radial pressure.

In the case of static disks without radial pressure, there are two common interpretations. The stability of these models can be explained by either assuming the existence of hoop stresses or that the particles on the disk plane move under the action of their own gravitational field in such a way that as many particles move clockwise as counter-clockwise. This last interpretation, the “Counter-Rotating Model” (CRM), is frequently made since it can be invoked to mimic true rotational effects. Even though this interpretation can be seen as a device, there are observational evidence of disks made of streams of rotating and counter-rotating matter [17, 18].

Disklike sources in presence of electromagnetic fields, specially magnetic fields, are also of astrophysical interest mainly in the study of neutron stars, white dwarfs and galaxy formation. In the context of general relativity models of disks for Kerr-Newman metrics [20], static axisymmetric spacetimes with magnetic fields [19] and conformastationary metrics [21], have been considered recently. Following the Ref. [20] the resulting disks can also be interpreted either as rings with internal pressure and currents or as two counter-rotating streams of freely moving charged particles, i.e. which move along electrogeodesics (solution to the geodesic equation in the presence of a Lorentz force).

The aim of this paper is to perform a detailed study of the CRM for generic electrostatic (magnetostatic) axially symmetric thin disks without radial pressure. The paper is organized as follows. In Sec. 2 we present a summary of the procedure to obtain thin disks models as rings with a purely azimuthal pressure and currents using the well-known “displace, cut and reflect” method extended to solutions of Einstein-Maxwell equations. In particular, we obtain expressions for the surface energy-momentum tensor and the electrostatic (magnetostatic) current density of the disk. Next, in Sec. 3, the disks are interpreted in terms of the CRM. We find a general constraint over the counter-rotating tangential velocities needed to cast the surface energy-momentum tensor of the disk as the superposition of two counter-rotating charged dust fluids. We then show that this constraint is satisfied if we take the two counter-rotating streams as circulating along electrogeodesics with equal and opposite tangential velocities. We also find explicit expressions for the energy densities, electrostatic (magnetostatic) current densities and velocities of the counter-rotating fluids. In following section, Secs. 4, three specific examples are considered based in simple solutions to the Einstein-Maxwell equations. The considered solutions are Reissner-Nordström in the electrostatic case, its magnetostatic counterpart, and two solutions generated from Taub-NUT and Kerr solutions. In particular, we study the tangential velocities, mass densities and electrostatic (magnetostatic) charge densities of both streams. Also the stability against radial perturbation is considered. Finally, in Sec. 5, we summarize our main results.

## 2 Static Relativistic Thin Disks

In this section we present a summary of the procedure to obtain electrostatic (magnetostatic) axially symmetric thin disks. The simplest metric to describe a static axially symmetric spacetime is the Weyl's line element

$$ds^2 = e^{-2\Phi}[r^2 d\varphi^2 + e^{2\Lambda}(dr^2 + dz^2)] - e^{2\Phi} dt^2, \quad (1)$$

where  $\Phi$  and  $\Lambda$  are functions of  $r$  and  $z$  only. The Einstein-Maxwell field equations, in geometrized units such that  $8\pi G = c = \mu_0 = \varepsilon_0 = 1$ , are given by

$$R_{ab} = T_{ab}, \quad (2a)$$

$$T_{ab} = F_{ac}F_b{}^c - \frac{1}{4}g_{ab}F_{cd}F^{cd}, \quad (2b)$$

$$F^{ab}{}_{;b} = 0, \quad (2c)$$

$$F_{ab} = A_{a,b} - A_{b,a}, \quad (2d)$$

where all symbols are understood. For the metric (1), the Einstein-Maxwell equations in presense of purely electric field are equivalent to the system

$$\Phi_{,rr} + \frac{1}{r}\Phi_{,r} + \Phi_{,zz} - \frac{e^{-2\Phi}}{2}(\psi_{,r}^2 + \psi_{,z}^2) = 0, \quad (3a)$$

$$\psi_{,rr} + \frac{1}{r}\psi_{,r} + \psi_{,zz} - 2(\Phi_{,r}\psi_{,r} + \Phi_{,z}\psi_{,z}) = 0, \quad (3b)$$

$$\Lambda_{,r} = r(\Phi_{,r}^2 - \Phi_{,z}^2) - \frac{re^{-2\Phi}}{2}(\psi_{,r}^2 - \psi_{,z}^2), \quad (3c)$$

$$\Lambda_{,z} = 2r\Phi_{,r}\Phi_{,z} - re^{-2\Phi}\psi_{,r}\psi_{,z}, \quad (3d)$$

and in the magnetostatic case to

$$\Phi_{,rr} + \frac{1}{r}\Phi_{,r} + \Phi_{,zz} - \frac{e^{2\Phi}}{2r^2}(A_{,r}^2 + A_{,z}^2) = 0, \quad (4a)$$

$$A_{,rr} - \frac{1}{r}A_{,r} + A_{,zz} + 2(A_{,r}\Phi_{,r} + A_{,z}\Phi_{,z}) = 0, \quad (4b)$$

$$\Lambda_{,r} = r(\Phi_{,r}^2 - \Phi_{,z}^2) + \frac{e^{2\Phi}}{2r}(A_{,r}^2 - A_{,z}^2), \quad (4c)$$

$$\Lambda_{,z} = 2r\Phi_{,r}\Phi_{,z} + \frac{1}{r}e^{2\Phi}A_{,r}A_{,z}, \quad (4d)$$

where  $\psi$  and  $A$  are the magnetostatic and electrostatic potential, respectively, which are also functions of  $r$  and  $z$ .

In order to obtain a solution of (4) - (3) representing a thin disc at  $z = 0$ , we assume that the components of the metric tensor are continuous across the disk, but their discontinuous first derivatives on plane  $z = 0$ , with discontinuity functions

$$b_{ab} = g_{ab,z}|_{z=0^+} - g_{ab,z}|_{z=0^-} = 2 g_{ab,z}|_{z=0^+} .$$

Thus, the Einstein-Maxwell equations yield an energy-momentum tensor  $T_a^b = Q_a^b \delta(z)$  and a planar current density  $i^a = 2F^{az}\delta(z)$ , where  $\delta(z)$  is the usual Dirac function with support on the disk and

$$Q_b^a = \frac{1}{2} \{ b^{az} \delta_b^z - b^{zz} \delta_b^a + g^{az} b_b^z - g^{zz} b_b^a + b_c^c (g^{zz} \delta_b^a - g^{az} \delta_b^z) \}$$

is the distributional energy-momentum tensor. The “true” surface energy-momentum tensor (SEMT) of the disk,  $S_a^b$ , can be obtained through the relation

$$S_a^b = \int T_a^b ds_n = e^{\Lambda-\Phi} Q_a^b , \quad (5)$$

where  $ds_n = \sqrt{g_{zz}} dz$  is the “physical measure” of length in the direction normal to the disk, and the current density as  $j^a = e^{\Lambda-\Phi} i^a$ . For the metric (1), the non-zero components of  $S_a^b$  are

$$S_0^0 = 2e^{\Phi-\Lambda} \{ \Lambda_{,z} - 2\Phi_{,z} \} , \quad (6a)$$

$$S_1^1 = 2e^{\Phi-\Lambda} \Lambda_{,z} , \quad (6b)$$

and current density equal to

$$j_t = -2e^{\Phi-\Lambda} \psi_{,z} , \quad (7a)$$

$$j_\varphi = -2e^{\Phi-\Lambda} A_{,z} , \quad (7b)$$

in the electrostatic and magnetostatic cases, respectively. All the quantities are evaluated at  $z = 0^+$ .

With an orthonormal tetrad  $e_a^b = \{V^b, W^b, X^b, Y^b\}$ , where

$$V^a = e^{-\Phi} (1, 0, 0, 0) , \quad (8a)$$

$$W^a = \frac{e^\Phi}{r} (0, 1, 0, 0) , \quad (8b)$$

$$X^a = e^{\Phi-\Lambda} (0, 0, 1, 0) , \quad (8c)$$

$$Y^a = e^{\Phi-\Lambda} (0, 0, 0, 1) , \quad (8d)$$

we can write the metric and the SEMT in the canonical forms

$$g_{ab} = -V_a V_b + W_a W_b + X_a X_b + Y_a Y_b, \quad (9a)$$

$$S_{ab} = \epsilon V_a V_b + p_\varphi W_a W_b, \quad (9b)$$

where

$$\epsilon = -S_0^0, \quad p_\varphi = S_1^1, \quad (10)$$

are, respectively, the energy density and the azimuthal pressure of the disk.

### 3 The Counter-Rotating Model

We now consider, based on references [22] and [23], the possibility that the SEMT  $S^{ab}$  and the current density  $j^a$  can be written as the superposition of two counter-rotating fluids that circulate in opposite directions; that is, we assume

$$S^{ab} = S_+^{ab} + S_-^{ab}, \quad (11a)$$

$$j^a = j_+^a + j_-^a, \quad (11b)$$

where the quantities in the right-hand side are, respectively, the SEMT and the current density of the prograd and retrograd counter-rotating fluids.

Let  $U_\pm^a = (U_\pm^0, U_\pm^1, 0, 0)$  be the velocity vectors of the two counter-rotating fluids. In order to do the decomposition (11a) and (11b) we project the velocity vectors onto the tetrad  $e_{\hat{a}}^b$ , using the relations [24]

$$U_\pm^{\hat{a}} = e_{\hat{b}}^a U_\pm^b, \quad U_\pm^a = U_\pm^{\hat{c}} e_{\hat{c}}^a. \quad (12)$$

With the tetrad (8) we can write

$$U_\pm^a = \frac{V^a + U_\pm W^a}{\sqrt{1 - U_\pm^2}}, \quad (13)$$

and thus

$$V^a = \frac{\sqrt{1 - U_-^2} U_+ U_-^a - \sqrt{1 - U_+^2} U_- U_+^a}{U_+ - U_-}, \quad (14a)$$

$$W^a = \frac{\sqrt{1 - U_+^2} U_+^a - \sqrt{1 - U_-^2} U_-^a}{U_+ - U_-}, \quad (14b)$$

where  $U_\pm = U_\pm^1 / U_\pm^0$  are the tangential velocities of the fluids with respect to the tetrad.

Using (14), we can write the SEMT as

$$\begin{aligned}
S^{ab} &= \frac{f(U_-, U_-)(1 - U_+^2) U_+^a U_+^b}{(U_+ - U_-)^2} \\
&+ \frac{f(U_+, U_+)(1 - U_-^2) U_-^a U_-^b}{(U_+ - U_-)^2} \\
&- \frac{f(U_+, U_-)(1 - U_+^2)^{\frac{1}{2}}(1 - U_-^2)^{\frac{1}{2}}(U_+^a U_-^b + U_-^a U_+^b)}{(U_+ - U_-)^2},
\end{aligned}$$

where

$$f(U_1, U_2) = \epsilon U_1 U_2 + p_\varphi. \quad (15)$$

Clearly, in order to cast the SEMT in the form (11a), the mixed term must be absent and therefore the counter-rotating tangential velocities must be related by

$$f(U_+, U_-) = 0, \quad (16)$$

where we assume that  $|U_\pm| \neq 1$ . Then, assuming a given choice for the counter-rotating velocities in agreement with the above relation, we can write the SEMT as (11a) with

$$S_\pm^{ab} = \epsilon_\pm U_\pm^a U_\pm^b, \quad (17)$$

so that we have two counter-rotating dust fluids with energy densities given by

$$\epsilon_\pm = \left[ \frac{1 - U_\pm^2}{U_\mp - U_\pm} \right] U_\mp \epsilon. \quad (18)$$

Thus the SEMT  $S^{ab}$  can be written as the superposition of two counter-rotating dust streams if, and only if, the constraint (16) admits a solution such that  $U_+ \neq U_-$ . This result is completely equivalent to the necessary and sufficient condition obtained in reference [23].

Similarly, we can write the current density in both cases as (11b) with

$$\mathbf{j}_\pm^a = \sigma_\pm U_\pm^a, \quad (19)$$

where  $\sigma_\pm$  are the counter-rotating rest-charge densities of the fluids which are given by

$$\sigma_{e\pm} = \frac{J^0}{V^0} \left[ \frac{\sqrt{1 - U_\pm^2}}{U_\mp - U_\pm} \right] U_\mp, \quad (20a)$$

$$\sigma_{m\pm} = \frac{J^1}{W^1} \left[ \frac{\sqrt{1 - U_\pm^2}}{U_\pm - U_\mp} \right], \quad (20b)$$

respectively. Note that the counter-rotating energy densities  $\epsilon_{\pm}$  and electrostatic (magnetostatic) charge densities  $\sigma_{e\pm}(\sigma_{m\pm})$  are not uniquely defined by the above relations, also for definite values of  $U_{\pm}$ .

Another quantity related with the counter-rotating motion is the specific angular momentum of a particle rotating at a radius  $r$ , defined as  $h_{\pm} = g_{\varphi\varphi}U_{\pm}^{\varphi}$ . We can write

$$h_{\pm} = \frac{re^{-\Phi}U_{\pm}}{\sqrt{1-U_{\pm}^2}}. \quad (21)$$

This quantity can be used to analyze the stability of the disks against radial perturbations. The condition of stability,

$$\frac{d(h^2)}{dr} > 0, \quad (22)$$

is an extension of Rayleigh criteria of stability of a fluid in rest in a gravitational field [25].

We shall now analyze the possibility of a complete determination of the vectors  $U_{\pm}^a$ . As we can see, the constraint (16) does not determine  $U_{\pm}$  uniquely, and so there is a freedom in the choice of  $U_{\pm}^a$ . A possibility, commonly assumed, is to take the two counter-rotating fluids as circulating along electro-geodesics

$$\frac{1}{2}\epsilon_{\pm}g_{ab,r}U_{\pm}^aU_{\pm}^b = -\sigma_{\pm}F_{ra}U_{\pm}^a. \quad (23)$$

Let  $\omega_{\pm} = U_{\pm}^1/U_{\pm}^0$  be the angular velocities of the particles. Using (13), (18) and (20a), in electrostatic case (23) takes the form

$$g_{11,r}\omega^2 + g_{00,r} = -\frac{2j^0V_0^2}{\epsilon}\psi_{,r}, \quad (24)$$

so that

$$\omega_{\pm} = \pm \omega, \quad \omega^2 = -\frac{g_{00,r}}{g_{11,r}} - \frac{2j^0V_0^2}{\epsilon g_{11,r}}\psi_{,r}, \quad (25)$$

and similarly, using (20b) instead of (20a) in magnetostatic case we obtain

$$g_{11,r}\omega^2 + g_{00,r} = -\frac{2j^1V_0^2}{\epsilon}A_{,r}, \quad (26)$$

so that

$$\omega_{\pm} = \pm \omega, \quad \omega^2 = -\frac{g_{00,r}}{g_{11,r}} - \frac{2j^1V_0^2}{\epsilon g_{11,r}}A_{,r}. \quad (27)$$

Note that in both cases, the two geodesic fluids circulate with equal and opposite velocities.

In order to see if the geodesic velocities agree with (16), we need to compute  $f(U_+, U_-)$ . In terms of  $\omega_{\pm}$  we get

$$U_{\pm} = \pm U = \pm \left[ \frac{V^0}{W^1} \right] \omega, \quad (28)$$

and so, using the Einstein-Maxwell equations (3) and (4) and the expressions (6a) - (7b) for the SEMT and the current density we can show that  $f(U_+, U_-)$  vanishes in both cases, so that the constraint (16) is equivalent to

$$U^2 = \frac{p_{\varphi}}{\epsilon}, \quad (29)$$

as is commonly assumed in the works concerning counter-rotating disks. We now have two counter-rotating charged dust streams with equal energy densities

$$\epsilon_{\pm} = \frac{\epsilon - p_{\varphi}}{2}, \quad (30)$$

specific angular momenta

$$h_{\pm} = r e^{-\Phi} \sqrt{\frac{p_{\varphi}}{\epsilon - p_{\varphi}}}, \quad (31)$$

charge densities

$$\sigma_{e\pm} = -\frac{1}{2} e^{-\Phi} j_0 \sqrt{1 - \frac{p_{\varphi}}{\epsilon}}, \quad (32a)$$

$$\sigma_{m\pm} = \frac{1}{2r} e^{\Phi} j_1 \sqrt{\frac{\epsilon}{p_{\varphi}} - 1}, \quad (32b)$$

and velocities given by (29). As we can see, in this case we have a complete determination of all the quantities involved in the CRM.

## 4 Some Simple CRM Models

### 4.1 CRM for Reissner-Nordström like disks

The simplest electrostatic solution of the Einstein- Maxwell equations is the well-known Reissner-Nordström solution [26], which can be written as (1) with

$$\Phi = \frac{1}{2} \ln \left[ \frac{x^2 - 1}{(x + a)^2} \right], \quad (33a)$$

$$\Lambda = \frac{1}{2} \ln \left[ \frac{x^2 - 1}{x^2 - y^2} \right], \quad (33b)$$

$$\psi = \frac{\sqrt{2}b}{x + a}, \quad (33c)$$



where  $a = m/k$ ,  $b = e/k$ , with  $k^2 = m^2 - e^2$ , so that  $a^2 = 1 + b^2$ . Here  $m$  and  $e$  are the mass and the charge, respectively.  $x$  and  $y$  are the prolate spheroidal coordinates, related to the Weyl coordinates by

$$2kx = \sqrt{r^2 + (z + z_0 + k)^2} + \sqrt{r^2 + (z + z_0 - k)^2}, \quad (34a)$$

$$2ky = \sqrt{r^2 + (z + z_0 + k)^2} - \sqrt{r^2 + (z + z_0 - k)^2}. \quad (34b)$$

Note that we have displaced the origin of the  $z$  axis in  $z_0$ . This solution can be generated, in these coordinates, using the well-known complex potential formalism proposed by Ernst [27, 28] from Schwarzschild solution [29]. Indeed for  $b = 0$ , it goes over into the Schwarzschild solution. Thus,  $b$  is the parameter governing the electric field. One can obtain its magnetostatic counterpart computing the magnetostatic potential via

$$A_{,x} = kf^{-1}(1 - y^2)\psi_{,y}, \quad (35a)$$

$$A_{,y} = -kf^{-1}(x^2 - 1)\psi_{,x}. \quad (35b)$$

Thus, we find

$$A = \sqrt{2}kby, \quad (36)$$

again with  $a^2 - b^2 = 1$ . From the above expressions we can compute the physical quantities associated with disk. We obtain

$$\tilde{\epsilon} = \frac{4\bar{y}(\bar{x}^2 - 1)(a\bar{x} + \bar{y}^2)}{(\bar{x} + a)^2(\bar{x}^2 - \bar{y}^2)^{3/2}}, \quad (37)$$

$$\tilde{p}_\varphi = \frac{4\bar{x}\bar{y}(1 - \bar{y}^2)}{(\bar{x} + a)(\bar{x}^2 - \bar{y}^2)^{3/2}}, \quad (38)$$

$$\tilde{j}_t = \frac{2\sqrt{2}b\bar{y}(\bar{x}^2 - 1)}{(\bar{x}^2 - \bar{y}^2)^{1/2}(\bar{x} + a)^3}, \quad (39)$$

$$j_\varphi = -\frac{2\sqrt{2}b\bar{x}(1 - \bar{y}^2)}{(\bar{x}^2 - \bar{y}^2)^{1/2}(\bar{x} + a)}, \quad (40)$$

where  $\tilde{\epsilon} = k\epsilon$ ,  $\tilde{p}_\varphi = kp_\varphi$  and  $\tilde{j}_t = kj_t$ .  $\bar{x}$  and  $\bar{y}$  are given by

$$2\bar{x} = \sqrt{\tilde{r}^2 + (\alpha + 1)^2} + \sqrt{\tilde{r}^2 + (\alpha - 1)^2}, \quad (41a)$$

$$2\bar{y} = \sqrt{\tilde{r}^2 + (\alpha + 1)^2} - \sqrt{\tilde{r}^2 + (\alpha - 1)^2}, \quad (41b)$$

where  $\tilde{r} = r/k$  and  $\alpha = z_0/k$ , with  $\alpha > 1$ .

In order to study the behavior of these quantities we perform a graphical analysis of them for disks with  $\alpha = 1.4$  and  $b = 0, 0.5, 1.0,$  and  $1.5$ . In Fig. 1(a) we show the energy density  $\tilde{\epsilon}$  as a function of  $\tilde{r}$ . We see that the energy density present a maximum at  $\tilde{r} = 0$  and then decreases rapidly with  $\tilde{r}$ . We also see that the presence of electric (magnetic) field decreases the energy density in the central regions of the disks and later increases it. For other values of  $\alpha$  and  $b$  we obtain a similar behavior.

In Fig. 1(b) we plot the azimuthal pressure  $\tilde{p}_\varphi$  as function of  $\tilde{r}$ . We can observe that the pressure increases rapidly as one moves away from the disk center, reaches a maximum and later rapidly decreases. Note that electric (magnetic) field decreases the pressure everywhere on the disk. For other values of  $\alpha$  and  $b$  we have a similar behavior.

The electrostatic current  $\tilde{j}_t$  is presented in Fig. 2(a). Similarly to the energy density, it has a maximum at the disk center and then decreases rapidly with  $\tilde{r}$ . For other values of  $\alpha$  and  $b$  we observe a similar behavior. In addition, the magnetostatic current  $j_\varphi$  is plotted in Fig. 2(b) as function also of  $\tilde{r}$ . As we can observe it has a similar behavior to the pressure.

We now consider the CRM for the same value of the parameters. All the significant quantities can also be expressed in analytic form from above expressions but the results are so cumbersome that it is best just to analyze them graphically. In Fig. 3(a) we show the velocity curves of counter-rotating streams  $U^2$  as functions of  $\tilde{r}$ . We observe that it increases rapidly in the central region of the disk, achieves a maximum and later decreases monotonly. We also see that the presence of electric (magnetic) field makes least relativistic the disks. In addition, in Fig. 3(b), we plot  $U^2$  for disks with  $b = 0.5$  and  $\alpha = 1.01, 1.1, 1.4,$  and  $2.0$ . We find that the disks become least relativistic with increasing  $\alpha$ . We also find that the disks with  $\alpha < 1$  cannot be built from CRM because  $U^2 > 1$  (not shown in the figure).

In Fig. 4(a) we have drawn the specific angular momentum  $\tilde{h}^2$  of counter-rotating fluids, where  $\tilde{h} = h_\pm/k$ . In the cases considered we obtain  $\tilde{h}^2$  as increasing monotonic functions of  $\tilde{r}$  what correspond to stable CRM for the disks. However, the CRM cannot be applied for  $b = 4.0$  (dotted curve). Thus the presence of electric (magnetic) field can makes unstable the CRM against radial perturbations. Finally, in Figs. 4(b) and 5 the plots of the mass densities  $\epsilon_\pm$  and electrostatic (magnetostatic) charge densities  $\sigma_{e\pm}(\sigma_{m\pm})$  of both streams are shown. These present a maximum at the disks center and then decrease monotonly. Therefore, the CRM constructed from this value of the parameters are well behaved.

## 4.2 CRM for Taub-NUT like disks

A Taub-NUT like solution to the Einstein-Maxwell equations is

$$\Phi = \ln \left[ \frac{x^2 - 1}{x^2 + 2ax + 1} \right], \quad (42a)$$

$$\Lambda = 2 \ln \left[ \frac{x^2 - 1}{x^2 - y^2} \right], \quad (42b)$$

$$\psi = \frac{2\sqrt{2}bx}{x^2 + 2ax + 1}, \quad (42c)$$

with  $a^2 - b^2 = 1$ .  $x$  and  $y$  are, again, the prolate spheroidal coordinates, given by Eqs. (34a) and (34b). This solution can also be generated, in these coordinates, using the well-known complex potential formalism proposed by Ernst [27, 28] from Weyl 2-solution (Darmois [26]). Indeed for  $b = 0$ , it goes over into the Darmois solution. Thus, again,  $b$  is the electric parameter. One can also obtain its magnetostatic counterpart computing the magnetostatic potential using (35), and we get

$$A = 2\sqrt{2}kby, \quad (43)$$

again with  $a^2 - b^2 = 1$ . The physical quantities associated with the disk now can be written as

$$\tilde{\epsilon} = \frac{8\bar{y}[\bar{x}(a\bar{x}^3 - 3a\bar{x} - 2) + \bar{y}^2(2\bar{x}^3 + 3a\bar{x}^2 - a)]}{(\bar{x}^2 - 1)(\bar{x}^2 + 2a\bar{x} + 1)^2}, \quad (44)$$

$$\tilde{p}_\varphi = \frac{16\bar{x}\bar{y}(1 - \bar{y}^2)}{(\bar{x}^2 - 1)(\bar{x}^2 + 2a\bar{x} + 1)}, \quad (45)$$

$$\tilde{j}_t = \frac{4\sqrt{2}b\bar{y}(\bar{x}^2 - 1)(\bar{x}^2 - \bar{y}^2)}{(\bar{x}^2 + 2a\bar{x} + 1)^3}, \quad (46)$$

$$j_\varphi = -\frac{4\sqrt{2}b\bar{x}(1 - \bar{y}^2)(\bar{x}^2 - \bar{y}^2)}{(\bar{x}^2 - 1)(\bar{x}^2 + 2a\bar{x} + 1)}, \quad (47)$$

where  $\bar{x}$  and  $\bar{y}$  are given by Eqs. (41a) and (41b).

In Figs. 6 and 7 the plots of the quantities  $\tilde{\epsilon}$ ,  $\tilde{p}_\varphi$ ,  $\tilde{j}_t$  and  $j_\varphi$  are presented for disks with  $\alpha = 2.5$  and  $b = 0, 0.5, 1.0$ , and  $1.5$ . We see that these disks have a similar behavior to the previous case. Equally, the relevant quantities of the CRM are shown in following figures for the same value of the parameters. Theses CRM are more relativistic than the ones built from Reissner-Nordström like solution (Fig. 8(a)). Note that (Fig. 8(b)) the disks with  $b = 0.5$   $\alpha = 1.5$  (solid curve) cannot be constructed from the CRM because  $U^2 > 1$ . We also note that the presence of electric (magnetic) field can makes unstable the CRM against radial perturbations (Fig. 9(a)). Thus the CRM cannot

apply for  $b = 3$  (dotted curve) . The remaining functions are plotted for the value of the parameters representing a physically acceptable CRM (Fig. 9(b) and 10). Also these have a similar behavior to the previous case.

### 4.3 CRM for Kerr like disks

A Kerr-like solution to the Einstein-Maxwell equations is

$$\Phi = \ln \left[ \frac{a^2 x^2 - b^2 y^2 - 1}{(ax + 1)^2 - b^2 y^2} \right], \quad (48a)$$

$$\Lambda = 2 \ln \left[ \frac{a^2 x^2 - b^2 y^2 - 1}{a^2 (x^2 - y^2)} \right], \quad (48b)$$

$$\psi = \frac{2\sqrt{2}by}{(ax + 1)^2 - b^2 y^2}, \quad (48c)$$

with  $a^2 - b^2 = 1$ .  $x$  and  $y$  are, again, the prolate spheroidal coordinates, given by Eqs. (34a) and (34b). This solution can be generated, in these coordinates, using a well-know theorem proposed by Bonnor [30, 31] from Kerr solution. The previous solution can also be obtained using this same theorem from Taub-NUT solution. For  $b = 0$ , it also goes over into the Darmois solution. Thus, again,  $b$  is the electric parameter. One can also obtain its magnetostatic counterpart computing the magnetostatic potential using (35), and gives

$$A = -\frac{\sqrt{2}kb(1 - y^2)(ax + 1)}{a(a^2 x^2 - b^2 y^2 - 1)}, \quad (49)$$

again with  $a^2 - b^2 = 1$ . This solution describes the field of a massive magnetic dipole. The physical quantities associated with disk now can be written as

$$\begin{aligned} \tilde{\epsilon} = & 8a^4 \bar{y} \{ (\bar{x}^2 - \bar{y}^2) [a(\bar{x}^2 - 1) [(a\bar{x} + 1)^2 + b^2 \bar{y}^2] - 2b^2 \bar{x}(a\bar{x} + 1)(1 - \bar{y}^2)] \\ & - 2\bar{x}(\bar{x}^2 - 1)(1 - \bar{y}^2) [(a\bar{x} + 1)^2 - b^2 \bar{y}^2] \} \\ & / (a^2 \bar{x}^2 - b^2 \bar{y}^2 - 1)^2 [(a\bar{x} + 1)^2 - b^2 \bar{y}^2]^2, \end{aligned} \quad (50)$$

$$\tilde{p}_\varphi = \frac{16a^4 \bar{x} \bar{y} (\bar{x}^2 - 1)(1 - \bar{y}^2)}{(a^2 \bar{x}^2 - b^2 \bar{y}^2 - 1)^2 [(a\bar{x} + 1)^2 - b^2 \bar{y}^2]}, \quad (51)$$

$$\tilde{j}_t = -\frac{4\sqrt{2}a^4 b (\bar{x}^2 - \bar{y}^2) \{ \bar{x}(1 - \bar{y}^2) [(a\bar{x} + 1)^2 + b^2 \bar{y}^2] - 2a\bar{y}^2 (a\bar{x} + 1)(\bar{x}^2 - 1) \}}{(a^2 \bar{x}^2 - b^2 \bar{y}^2 - 1) [(a\bar{x} + 1)^2 - b^2 \bar{y}^2]^3}, \quad (52)$$

$$j_\varphi = -\frac{2\sqrt{2}a^4 b \bar{y} (\bar{x}^2 - 1)(1 - \bar{y}^2) (\bar{x}^2 - \bar{y}^2) [(a\bar{x} + 1)(3a\bar{x} + 1) + b^2 \bar{y}^2]}{(a^2 \bar{x}^2 - b^2 \bar{y}^2 - 1)^3 [(a\bar{x} + 1)^2 - b^2 \bar{y}^2]}, \quad (53)$$

where  $\bar{x}$  and  $\bar{y}$  are given by Eqs. (41a) and (41b).

In figs. 11 and 12 the plots of the physical quantities describing the disks are shown for  $\alpha = 1.8$  and  $b = 0, 0.5, 1.0,$  and  $1.5$ . The energy density behaves in the opposite way to the previous cases. That is, near to the disk center it increases when the electric (magnetic) field is applied and decreases later. The other quantities have a similar behavior to the precedent cases. However, the electrostatic current after some  $r$  takes negative values. Likewise, the quantities corresponding to the CRM are shown in following figures for the same value of the of the parameters  $\alpha$  and  $b$ . Theses CRM are more relativistic than the ones above considered (Fig. 13(a)). Note that (Fig. 13(b)) the disks with  $b = 0.5$  and  $\alpha = 1.4$  (solid curve) cannot be constructed from the CRM because  $U^2 > 1$ . We also note that the presence of electric (magnetic) field can stabilize the CRM against radial perturbations (Fig. 14(a)). Therefore, only the CRM constructed with  $b = 1.0,$  and  $1.5$  are well behaved. Finally, the other functions are drawn for the same value of the parameters (Figs. 14(b) and 15).

## 5 Discussion

A detailed study of the Counter-Rotating Model for generic electrostatic (magnetostatic) axially symmetric thin disks without radial pressure was presented. A general constraint over the counter-rotating tangential velocities was found, needed to cast the surface energy-momentum tensor of the disk in such a way that it can be interpreted as the superposition of two counter-rotating charged dust fluids. The constraint found is completely equivalent to the necessary and sufficient condition obtained in reference [23]. We next showed that this constraint is satisfied if we take the two counter-rotating fluids as circulating along electrogeodesics with equal and opposite tangential velocities. We also have obtained explicit expressions for the energy densities, electrostatic (magnetostatic) current densities and velocities of the counter-rotating streams in terms of the energy density, azimuthal pressure and planar current density of the disk, that are also equivalent to the correspondig expressions in reference [23].

Three specific examples were considered in the present work based in simple solutions to the Einsteins-Maxwell equations generated by conventional solution-generating techniques [26]. We found that the CRM for Kerr-like disks are more relativistics than the ones obtained from Taub-NUT and Reissner-Nordström like solutions. We also saw that the presence of electric (magnetic) field can make unstable the CRM against radial perturbations in the case of Taub-NUT and Reissner-Nordström like disks, and conversely, stabilize the CRM in the case of Kerr-like disks. We also constructed some CRM with well defined counter-rotating tangential velocities and stable against radial perturbations.

On the other hand, the generalization of the Counter-Rotating Model presented here to the case with radial pressure is in consideration. Also, the generalization to rotating thin disks with or without radial pressure in presence of electromagnetic fields is being

considered.

## Acknowledgments

Gonzalo García R. wants to thank a Fellowship from Vicerrectoría Académica, Universidad Industrial de Santander.

## References

- [1] W. A. Bonnor and A. Sackfield, *Comm. Math. Phys.* 8, 338 (1968).
- [2] T. Morgan and L. Morgan, *Phys. Rev.* 183, 1097 (1969).
- [3] L. Morgan and T. Morgan, *Phys. Rev. D*2, 2756 (1970).
- [4] A. Chamorro, R. Gregory and J. M. Stewart, *Proc. R. Soc. Lond. A* 413, 251 (1987).
- [5] G. A. González and P. S. Letelier. *Class. Quantum. Grav.* 16, 479 (1999).
- [6] D. Lynden-Bell and S. Pineault, *Mon. Not. R. Astron. Soc.* 185, 679 (1978).
- [7] P.S. Letelier and S. R. Oliveira, *J. Math. Phys.* 28, 165 (1987).
- [8] J. P. S. Lemos, *Class. Quantum Grav.* 6, 1219 (1989).
- [9] J. P. S. Lemos and P. S. Letelier, *Class. Quantum Grav.* 10, L75 (1993).
- [10] J. Bičák, D. Lynden-Bell and J. Katz, *Phys. Rev. D*47, 4334 (1993).
- [11] J. Bičák, D. Lynden-Bell and C. Pichon, *Mon. Not. R. Astron. Soc.* 265, 126 (1993).
- [12] J. Bičák and T. Ledvinka. *Phys. Rev. Lett.* 71, 1669 (1993).
- [13] J. P. S. Lemos and P. S. Letelier, *Phys. Rev D*49, 5135 (1994).
- [14] J. P. S. Lemos and P. S. Letelier, *Int. J. Mod. Phys. D*5, 53 (1996).
- [15] C. Klein, *Class. Quantum Grav.* 14, 2267 (1997).
- [16] G. A. González and P. S. Letelier. *Phys. Rev. D* 62, 064025 (2000).
- [17] V. C. Rubin, J. A. Graham and J. D. P Kenney. *Ap. J.* 394, L9-L12, (1992).
- [18] H. Rix, M. Franx, D. Fisher and G. Illingworth. *Ap. J.* 400, L5-L8, (1992).

- [19] P. S. Letelier. Phys. Rev. D 60, 104042 (1999).
- [20] T. Ledvinka, J. Bičák, and M. Žofka, in *Proceeding of 8th Marcel-Grossmann Meeting in General Relativity*, edited by T. Piran (World Scientific, Singapore, 1999)
- [21] J. Katz, J. Bičák and D. Lynden-Bell, Class. Quantum Grav. 16, 4023 (1999).
- [22] P. S. Letelier. Phys. Rev. D 22, 807 (1980).
- [23] J. J. Ferrando, J. A. Morales and M. Portilla. Gen. Rel. and Grav. 22, 1021 (1990).
- [24] S. Chandrasekar, *The Mathematical Theory of Black Holes*. (Oxford University Press, 1992).
- [25] L. D. Landau and E. M. Lifshitz, *Fluid Mechanics* (Addison-Wesley, Reading, MA, 1989).
- [26] D. Kramer, H. Stephani, E. Herlt, and M. McCallum, *Exact Solutions of Einsteins's Field Equations* (Cambridge University Press, Cambridge, England, 1980).
- [27] F. J. Ernst. Phys. Rev. D 167, 1175 (1968).
- [28] F. J. Ernst. Phys. Rev. D 168, 1415 (1968).
- [29] K. Schwarzschild. Sitzungsber. Preuss. Akad. Wiss., 189 (1968).
- [30] W. B. Bonnor. Z. Phys. 161, 439 (1961).
- [31] W. B. Bonnor. Z. Phys. 190, 444 (1966).

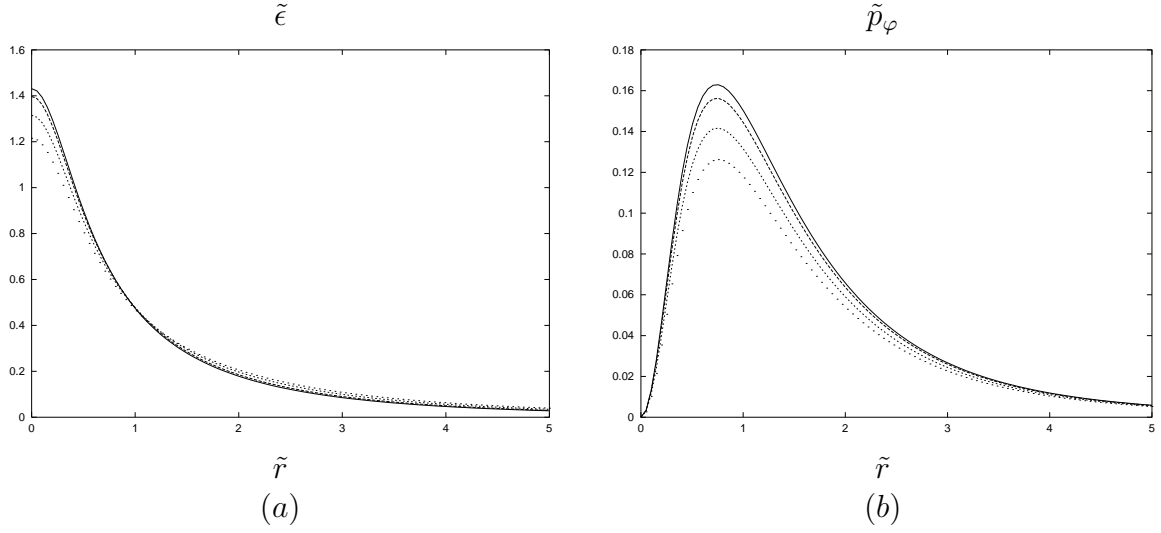


Figure 1: (a) Energy density  $\tilde{\epsilon}$  and (b) azimuthal pressure  $\tilde{p}_\varphi$  as functions of  $\tilde{r}$  for disks with  $\alpha = 1.5$  and  $b = 0$  (solid curve), 0.5, 1.0, and 1.5 (dotted curve).

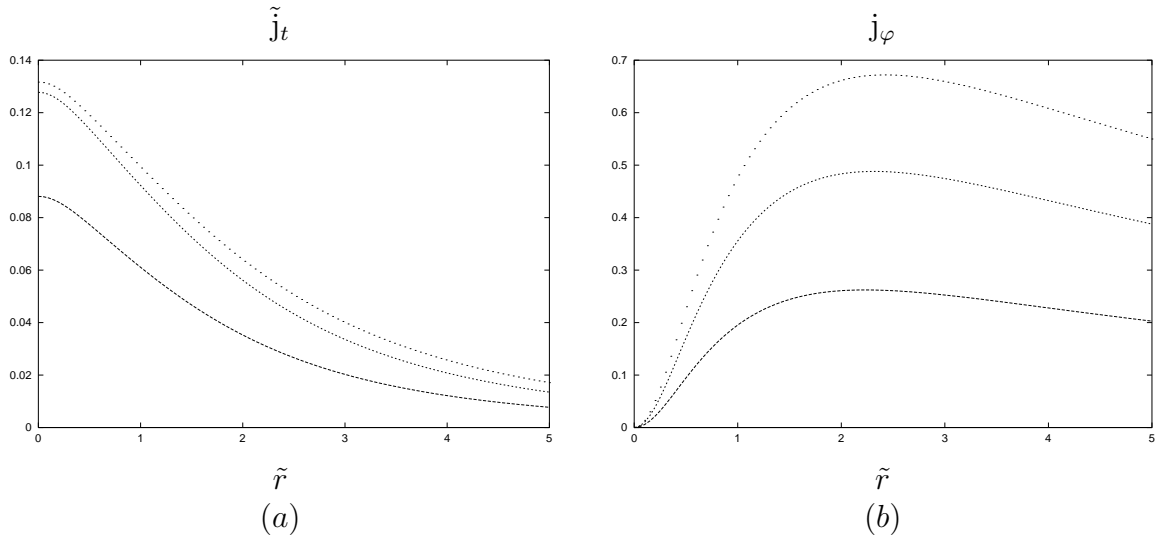


Figure 2: Surface current density: (a)  $\tilde{j}_t$  and (b)  $j_\varphi$  as functions of  $\tilde{r}$  for disks with  $\alpha = 1.5$  and  $b = 0$  (axis  $\tilde{r}$ ), 0.5, 1.0, and 1.5 (dotted curve).



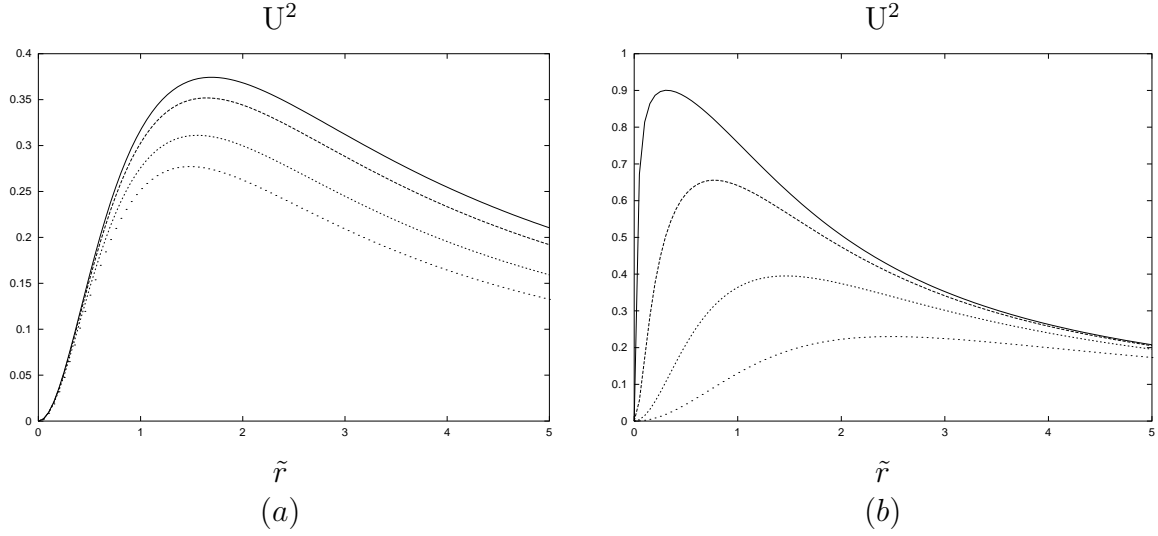


Figure 3: Tangential velocity  $U^2$  as function of  $\tilde{r}$  for disks with (a)  $\alpha = 1.5$  and  $b = 0$  (solid curve), 0.5, 1.0, and 1.5 (dotted curve), and (b)  $b = 0.5$  and  $\alpha = 1.01$  (solid curve), 1.1, 1.4, 2.0 (dotted curve)

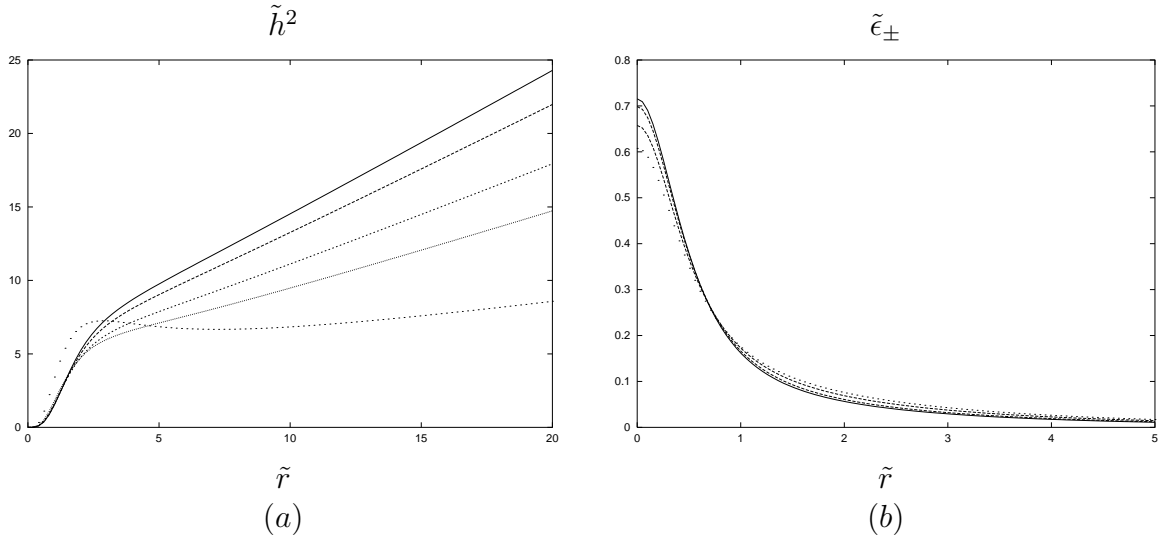


Figure 4: (a) Specific angular momentum  $\tilde{h}^2$  as function of  $\tilde{r}$  for disks with  $\alpha = 1.5$  and  $b = 0$  (solid curve), 0.5, 1.0, 1.5 and 4.0 (dotted curve). (b) Mass densities  $\tilde{\epsilon}_{\pm}$  as function of  $\tilde{r}$  for disks with  $\alpha = 1.5$  and  $b = 0$  (solid curve), 0.5, 1.0, and 1.5 (dotted curve).

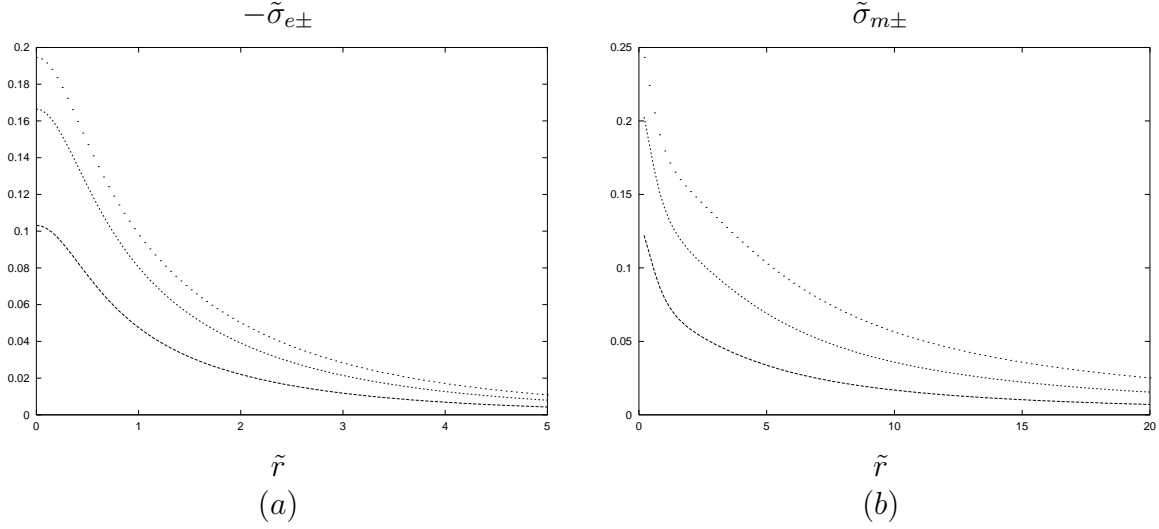


Figure 5: Charge densities: (a)  $\tilde{\sigma}_{e\pm}$  and (b)  $\tilde{\sigma}_{m\pm}$  as functions of  $\tilde{r}$  for disks with  $\alpha = 1.5$  and  $b = 0$  (axis  $\tilde{r}$ ), 0.5, 1.0, and 1.5 (dotted curve).

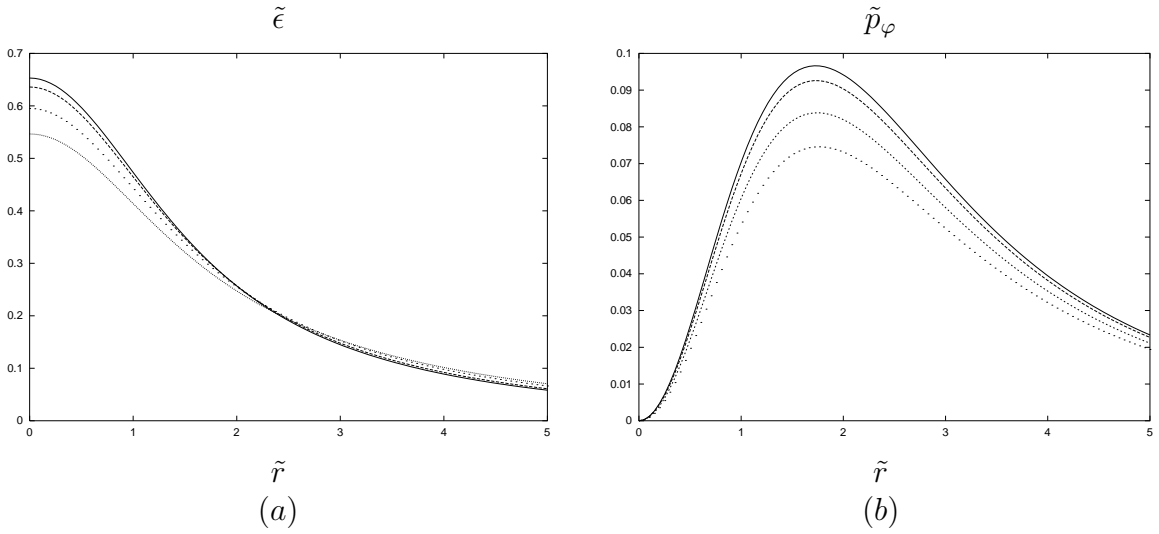


Figure 6: (a) Energy density  $\tilde{\epsilon}$  and (b) azimuthal pressure  $\tilde{p}_\varphi$  as functions of  $\tilde{r}$  for disks with  $\alpha = 2.5$  and  $b = 0$  (solid curve), 0.5, 1.0, and 1.5 (dotted curve).

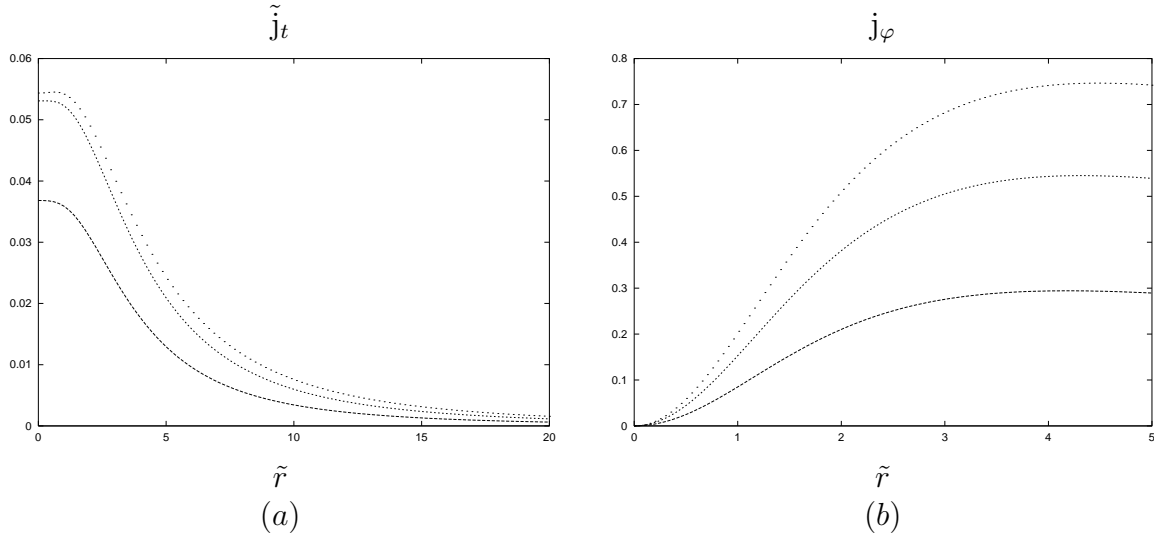


Figure 7: Planar current density: (a)  $\tilde{j}_t$  and (b)  $j_\varphi$  as functions of  $\tilde{r}$  for disks with  $\alpha = 2.5$  and  $b = 0$  (axis  $\tilde{r}$ ), 0.5, 1.0, and 1.5 (dotted curve).

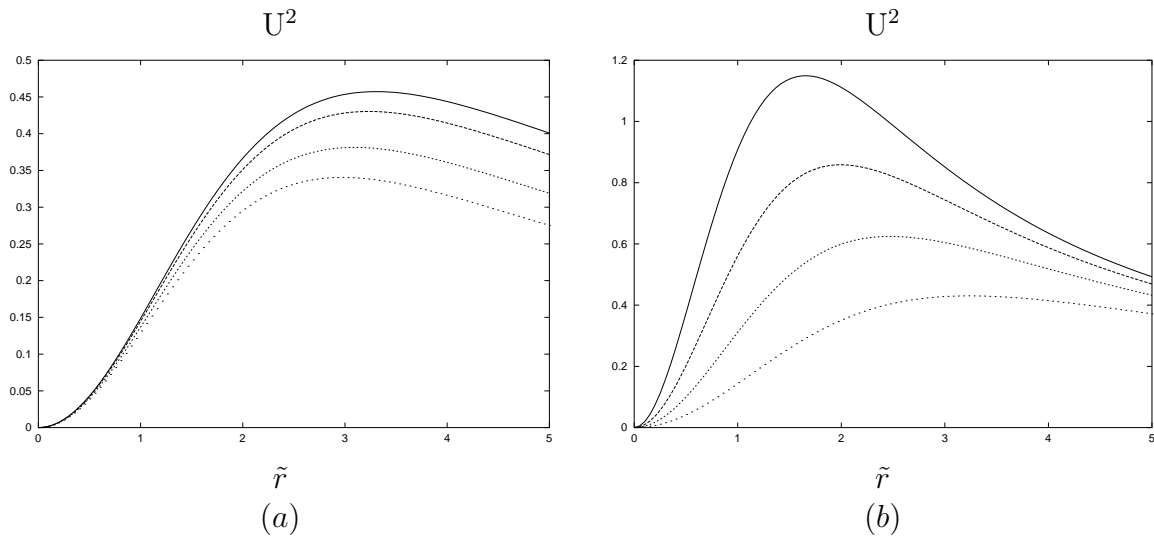


Figure 8: Tangential velocity  $U^2$  as function of  $\tilde{r}$  for disks with (a)  $\alpha = 2.5$  and  $b = 0$  (solid curve), 0.5, 1.0, and 1.5 (dotted curve), and (b)  $b = 0.5$  and  $\alpha = 1.5$  (solid curve), 1.7, 2.0, 2.5 (dotted curve)

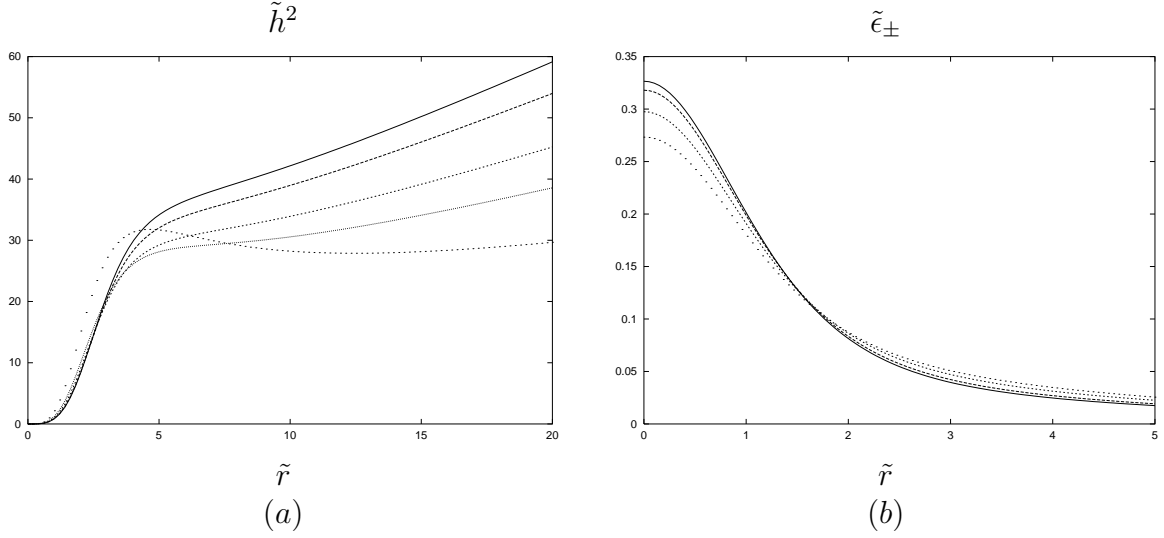


Figure 9: (a) Specific angular momentum  $\tilde{h}^2$  as function of  $\tilde{r}$  for disks with  $\alpha = 2.5$  and  $b = 0$  (solid curve), 0.5, 1.0, 1.5, and 3.0 (dotted curve). (b) Mass densities  $\tilde{\epsilon}_{\pm}$  as function of  $\tilde{r}$  for disks with  $\alpha = 2.5$  and  $b = 0$  (solid curve), 0.5, 1.0, and 1.5 (dotted curve).

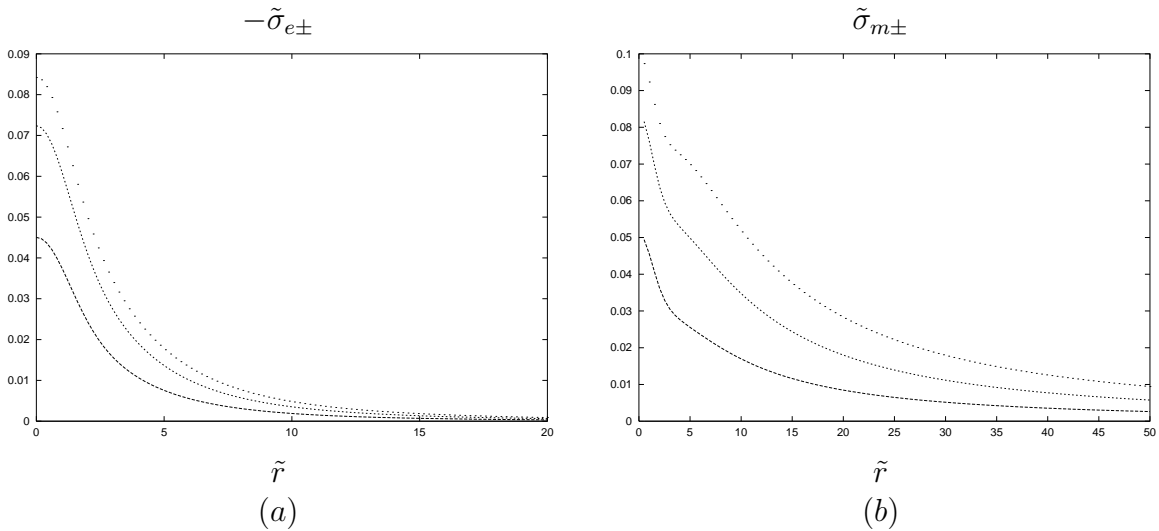


Figure 10: Charge densities: (a)  $\tilde{\sigma}_{e\pm}$  and (b)  $\tilde{\sigma}_{m\pm}$  as functions of  $\tilde{r}$  for disks with  $\alpha = 2.5$  and  $b = 0$  (axis  $\tilde{r}$ ), 0.5, 1.0, and 1.5 (dotted curve).

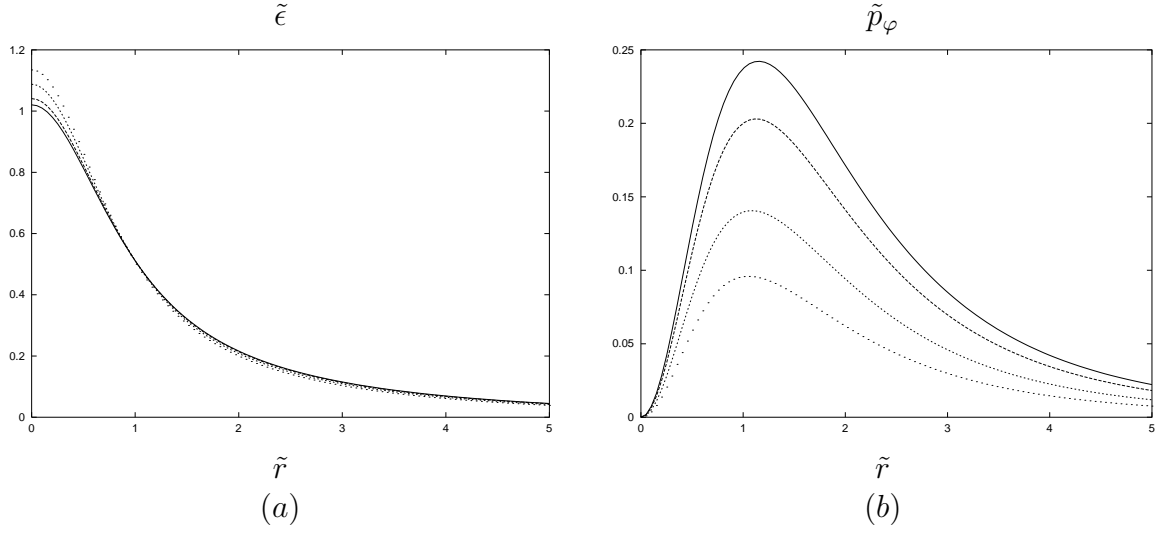


Figure 11: (a) Energy density  $\tilde{\epsilon}$  and (b) azimuthal pressure  $\tilde{p}_\varphi$  as functions of  $\tilde{r}$  for disks with  $\alpha = 1.8$  and  $b = 0$  (solid curve), 0.5, 1.0, and 1.5 (dotted curve).

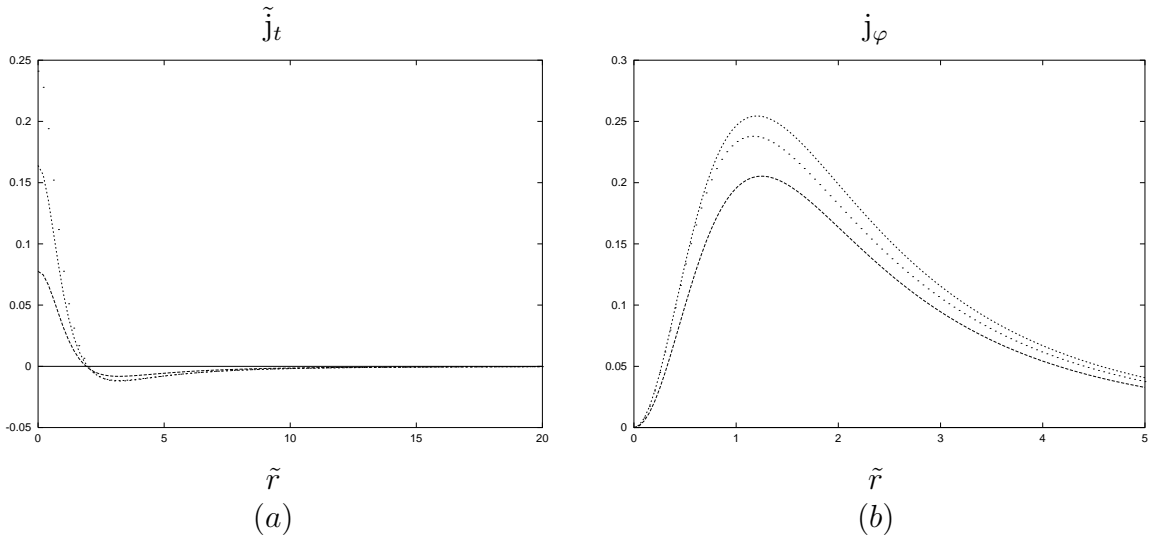


Figure 12: Current density: (a)  $\tilde{j}_t$  and (b)  $j_\varphi$  as functions of  $\tilde{r}$  for disks with  $\alpha = 1.8$  and  $b = 0$  (axis  $\tilde{r}$ ), 0.5, 1.0, and 1.5 (dotted curve).

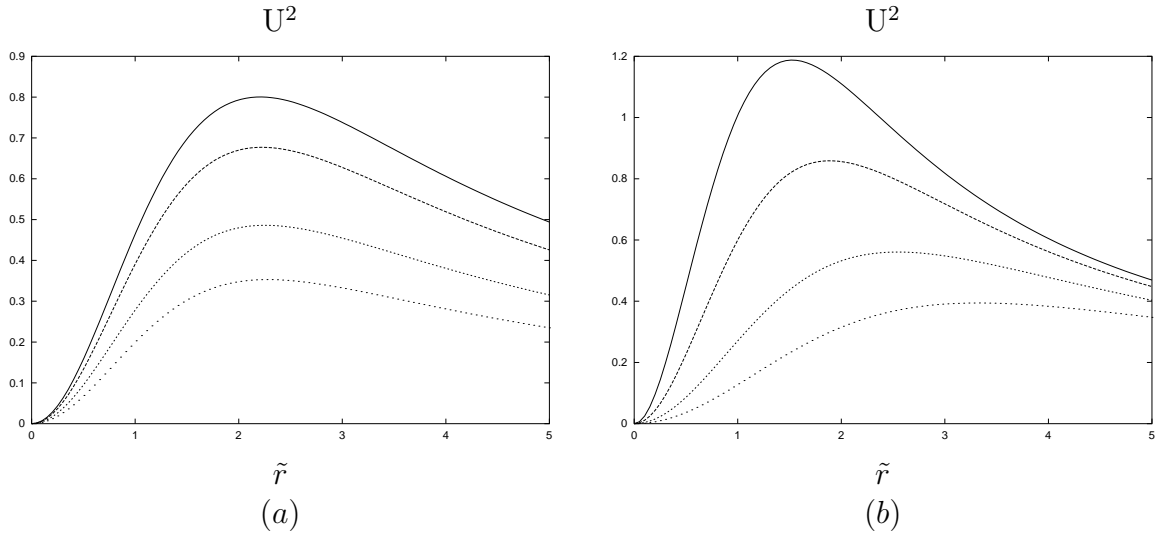


Figure 13: Tangential velocity  $U^2$  as function of  $\tilde{r}$  for disks with (a)  $\alpha = 1.8$  and  $b = 0$  (solid curve), 0.5, 1.0, and 1.5 (dotted curve), and (b)  $b = 0.5$  and  $\alpha = 1.4$  (solid curve), 1.6, 2.0, and 2.5 (dotted curve)

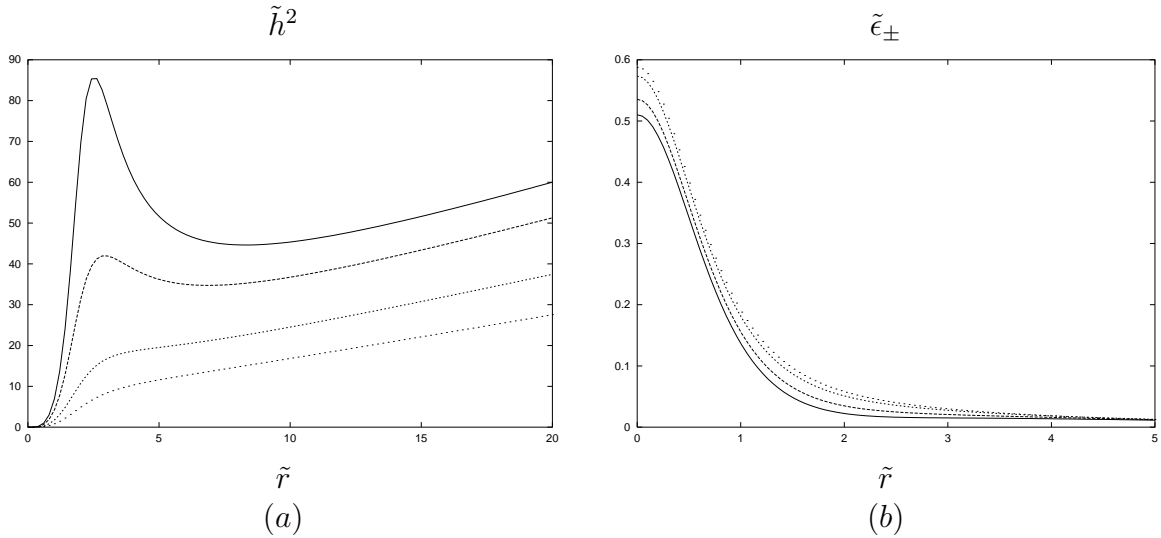


Figure 14: (a) Specific angular momentum  $\tilde{h}^2$  and (b) mass densities  $\tilde{\epsilon}_{\pm}$  as functions of  $\tilde{r}$  for disks with  $\alpha = 1.8$  and  $b = 0$  (solid curve), 0.5, 1.0, and 1.5 (dotted curve).

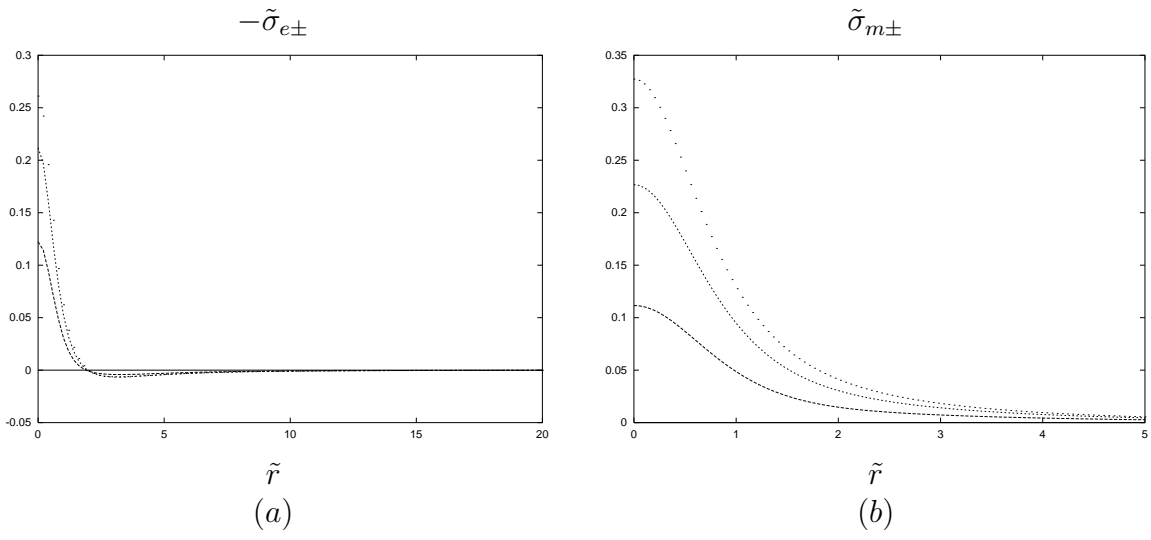


Figure 15: Charge densities: (a)  $\tilde{\sigma}_{e\pm}$  and (b)  $\tilde{\sigma}_{m\pm}$  as functions of  $\tilde{r}$  for disks with  $\alpha = 1.8$  and  $b = 0$  (axis  $\tilde{r}$ ), 0.5, 1.0, and 1.5 (dotted curve).